Transport properties of copper with excited electron subsystem

2016 J. Phys.: Conf. Ser. 774 012103

(http://iopscience.iop.org/1742-6596/774/1/012103)

Transport properties of copper with excited electron subsystem

Yu V Petrov[1,2], K P Migdal[1,3], D V Knyazev[2,4,5], N A Inogamov[1,3] and P R Levashov[4,6]

[1] Landau Institute for Theoretical Physics of the Russian Academy of Scienses, Akademika Semenova 1a, Chernogolovka, Moscow Region 142432, Russia
[2] Moscow Institute of Physics and Technology, Institutskiy Pereulok 9, Dolgoprudny, Moscow Region 141700, Russia
[3] Dukhov Research Institute of Automatics (VNIIA), Sushchevskaya 22, Moscow 127055, Russia
[4] Joint Institute for High Temperatures of the Russian Academy of Sciences, Izhorskaya 13 Bldg 2, Moscow 125412, Russia
[5] State Scientific Center of the Russian Federation "Institute for Theoretical and Experimental Physics", National Research Center "Kurchatov Institute", Bolshaya Cheremushkinskaya 25, Moscow 117218, Russia
[6] Tomsk State University, Lenina Avenue 36, Tomsk 634050, Russia

E-mail: migdal@vniia.ru

Abstract. We have investigated transport properties of an electron subsystem of copper heated by a femtosecond laser pulse. These properties change greatly in comparison with the room temperature solid metal. The electron temperature and pressure profiles significantly depend on these properties in bulk laser targets according to the two-temperature (2T) model. These profiles at the 2T stage are responsible for shock and rarefaction waves' formation. We have developed the analytical model of electroconductivity and heat conductivity of copper which takes into account changes of density, electron and ion temperatures. The model is based on the solution of the Boltzmann equation in the relaxation time approximation for consideration of electron collisions. Also we have carried out the first-principles calculations using the Kubo–Greenwood theory, methods of pseudopotential and linear augmented plane waves which are necessary to evaluate electron wavefunctions. We have provided the check of convergence of all parameters of our first-principles calculations. The results of our analytical model for electro- and heat conductivities are in good agreement with the data obtained using the linearized augmented plane wave (LAPW) method.

1. Introduction

Some years ago experimental investigations of ultrashort laser irradiation of copper and gold foils with submicrometer thickness have been provided [1,2]. In this case, thicknesses of foils and heated layer where two-temperature state is observed, have the same order of magnitude. Due to this, electron transport of energy to the cold bulk of the laser target is lacked. Thus the rate of laser energy relaxation is lower than for bulk laser targets. We can expect that maximum of electron temperature and duration of two-temperature state would be greater than for the case of bulk target. So we can say that accurate determination of electron thermodynamic and transport properties is an important task for the theoretical investigations of laser irradiation of these

targets. In the work [3], the experimental and first-principle investigations of copper transport properties were provided but only for low density range (0.3–0.5 g/cc). Using the analytical methods and first-principles calculations we consider a wide range of copper thermodynamic states which can exist after femtosecond irradiation by a laser pulse with fluence at the ablation threshold or slightly above. The range of considered densities was within the interval from 7.6 to 9.4 g/cc. Upper ion temperature was set equal to 15 000 K, the maximum electron temperature is 55 kK.

One of the most important questions discussed in this article is a description of the contribution of electron-electron collisions in quantum molecular dynamics calculations of the electronic kinetic coefficients in the approach based on the Kubo–Greenwood theory. Currently, this question is widely discussed, and there is no reliable answer. There are results of research carried out for simple metals [4] and hydrogen [5], where this influence is found to be negligible for normal densities. However, it is known that the above substances can be successfully considered in the model of almost free electrons because of the simplicity of their band structure, which actually does not change with electronic temperature. This is not true for the copper, containing a d-electron band not far from the Fermi energy, which according to available data [6] changes its position relative to the Fermi energy. It will be seen that the effect of electron-electron collisions is a factor that may explain the difference between data of first-principles calculations and independently constructed semi-analytical models.

Adequate evaluation of the thermal conductivity of the considered metal is necessary to carry out calculations by the method of two-temperature hydrodynamics, taking into account that this value is dependent on the density of the material and its electron and ion temperatures. To this date there were three main methods of calculation of heat conductivity.

The first one was to use a phenomenological dependencies [7, 8] obtained with the help of extrapolation of known data in some range of parameters of matter, such as temperature and density. In the second case, the main effort in determining the thermal conductivity was made to calculate the electron-electron collision frequencies to use them within the framework of relaxation time approximation [9–11]. The method of quantum molecular dynamics in combination with the Kubo–Greenwood theory provides an ability to calculate beyond the limitations of the aforementioned approaches. This method is the third approach to determine the behavior of electronic kinetic coefficients. This approach is used to calculate the kinetic coefficients in melts of metals over the past 15 years [12–15]. It can be noted that these papers were focused on the aluminum because of its simple electronic structure that diminishes the computational difficulty of the discussed problem.

The work [14] is an example of work where kinetic coefficients for metals with more complex electronic structure were calculated by using of the method of quantum molecular dynamics in combination with the Kubo–Greenwood formula. In this work, devoted in particular to the calculation of thermal conductivity, liquid gold with electrons, heated to temperatures of the order of several eV, was considered firstly. Gold has a fully filled d-band with a top, which lies in 2 eV below the Fermi energy, at low electronic temperatures. If the electron temperature is comparable to the gap between d-band and the Fermi energy, the electrons of this band becomes involved in the processes of absorption of laser energy and transfer it into the metal because of the thermal excitation of electrons into the unfilled states above the Fermi energy. Hence, it is necessary to take into account all eleven electrons of the valence bands for such a metal to describe electron kinetic coefficients using the method of quantum molecular dynamics in combination with the Kubo–Greenwood formula. This obstacle greatly complicates the task in comparison to the case of aluminum which has 3 valence electrons and gives the electronic structure which is similar to the one for free electron gas.

In this article the following section describes the main details of the approach used to calculate the kinetic coefficients of the copper. In the third section, we provided the initial data of our

calculation and also discussed the form of analytic fits we obtained to use them in our further calculations. The fourth section describes the semi-analytical model, based on the solution of the Boltzmann equation in the relaxation time approximation, the asymptotic dependencies for the thermal conductivity at low and high temperatures, as well as a simple model equation of state of heated metal. Consideration about the influence of electron-electron collisions on the result obtained using first-principles calculations is given in the fifth section. Comparison of the results obtained independently using the method of quantum molecular dynamics (QMD) and the Kubo–Greenwood formula on the one hand and with the use of semi-analytical models, on the other, is given in the sixth section. The discussion of calculated data for the thermal conductivity and resistivity and the comparison with experimental data and calculations based on the wide-range plasma models, are provided here.

2. Computational details

QMD simulations are widely used for calculations of properties of metals in a two-temperature state [16–21]. In this work, the calculation of the ionic configuration of copper in solid and liquid states was carried out using a QMD simulation for a supercell under periodic boundary conditions to reproduce the arrangement of atoms in condensed matter. The supercell contains 32 atoms in a cubic cell of size $2 \times 2 \times 2$ lattice periods for a given density. The description of the behavior of electrons was produced using PAW method and the exchange-correlation (xc) functional in the PBE form. DFT code VASP [22, 23] was used in the calculation of thermodynamic properties and ionic configurations. We have used the cutoff energy 300 eV, 15 empty levels per atom, and the magnitude of the error at convergence of electronic iterations was no more than a 10^{-5} eV for the total energy of the whole system. We use only 1 k-point located in Γ-point of the Brillouin zone of the supercell with 32 atoms.

To obtain ion configurations, QMD simulations were carried out in several stages by the use of different thermodynamic ensembles. In the first approach, the simulations were carried out for obtaining a phase state, predicted by the one-temperature phase diagram of the copper [25]. There three stages were carried out for modeling of the motion of atoms in the unit cell. At the first stage, we used the Nose–Hoover thermostat in the system during 1.5 ps, so that the ion temperature was raised up to the 4000 K, which is sufficient to obtain a melt according to a known one-temperature melting curve for all considered densities. In the second stage during also 1.5 ps the supercell in the liquid state is brought to the target temperature. Here, 7 values of ion temperature in the supercells were considered: 1, 2, 4, 7.5, and 15 kK. The values of the considered electron temperature in addition to the aforementioned ion temperatures are also included points 30 and 55 kK. Thus, only for the temperature 1 kK (and also 2 kK if the density is equal to 9.4 g/cc) the resulting state could not been the target, since these points lie either below the melting curve, or close to it. After bringing the atoms to a state with pair-correlation function corresponding to the molten copper, the thermostat was disconnected and the system was simulated in NVE ensemble.

In the second approach the necessity for the state initially stable according to the one-temperature phase diagram was ignored, so heating by the thermostat was carried out for the 3 ps to a state with the target temperature. Further, the stage of ionic configurations relaxation was held in the NVE ensemble, completely similar to the first approach. This stage has lasted for 0.5 ps.

The decision to hold this additional calculation with the use of the second approach stemmed from two reasons. First, we consider ultrashort processes in which the stable phase state, strictly speaking, is incorrect because stability of the phase state for such a short time cannot be determined. In such processes which are relevant on the time of electron-ion relaxation, heating of ion subsystem occurs monotonically, which is correspond to the calculation according to the second approach. Secondly, the pressure emerging in cell due to the strong electron heating

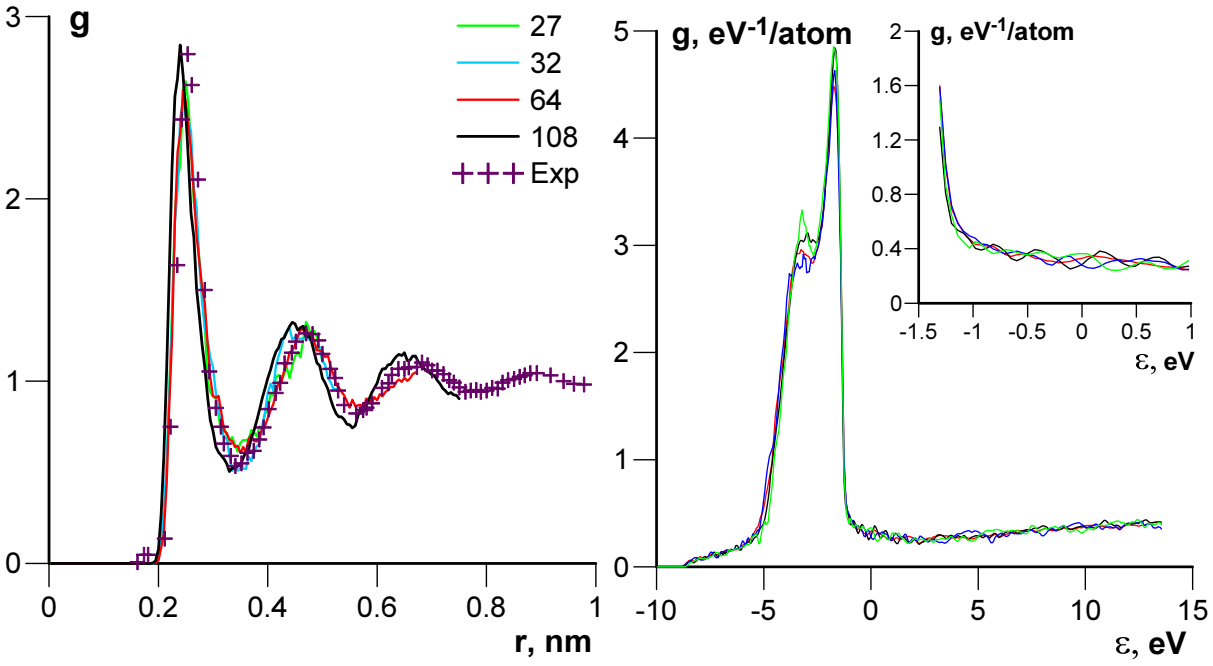

Figure 1. (a) Radial distribution function for the sets of ionic configurations with 108 (black), 64(blue), 32(red) and 27 (green) atoms of copper at the density of 8 g/cc and equilibrium temperature 2000 K. The experimental data were obtained by [24] for copper at 1473 K and atmospheric pressure. (b) Ion configuration averaged densities of states. The black, blue, red and green lines correspond to the supercells with 108, 64, 32 and 27 atoms. Densities of states around Fermi energy are shown in better resolution in the sidebar. The thermodynamic state is the same as in the left figure.

(up to several eV) for a fixed volume reaches the value 100 GPa and above. It can modify the behavior of the melting curve. For this reason, we have to talk about not only the melting curve, but the set of such curves for different fixed electronic temperatures.

The check was conducted to verify convergence in the number of particles in the calculations by full-electron approach, to see the influence of particle number of the ion distribution and electron spectra. In figure 1a there are presented pair-correlation function (PCF) of copper obtained by averaging over the set of 4 configurations for the calculation of systems containing 108, 64, 32 and 27 atoms. Five hundred ionic configurations were used for each number of atoms to calculate PCF with periodic boundary conditions. PCF are shown in figure 1a correspond to the thermodynamic state of copper at a density of 8 g/cc and the temperature of electrons and ions 2 kK. The experimental data shown in this figure were presented in work [24] for copper at atmospheric pressure and equilibrium temperature 1400 K which is close to melting point of copper (1356 K). We can notice that the density at the melting point for copper is the same as one used in our calculations of PCF presented in fig 1a. Thus, our results for PCF are in qualitative agreement with the experimental data despite of the noticeable difference between the temperature of measured state of copper and the temperature of state simulated by QMD. In the same way the averaged electron DoS was obtained for the indicated supercells with different number of atoms and the same temperature and density. According to PCF data, we can say that the calculation of the systems of 32 and 27 atoms give the possibility to describe only the first two peaks of PCF for liquid copper at given density and temperature. But even with 108 atoms the described range of PCF is limited to less than 1 nm. Data for DoS are shown in

Table 1. The convergence of the results obtained using pseudopotential approach in Kubo–Greenwood calculations for the state with density 9.4 g/cc, electron temperature $T_e = 55$ kK, and ion temperature $T_i = 7.5$ kK.

N_{at}	N_b	E_{cut}, eV	N_{kpt}	κ, W/(m K)	$\delta\kappa$, %	r, μOhm m	δr, %
32	11	300	64	2401	2.6	0.513	3
32	19	300	64	2450	6.4	0.522	4.5
32	11	600	64	2655	2.9	0.493	2.9
108	11	300	64	1179	6.3	0.464	4.4

Table 2. The convergence in the number of k-points for FP-LAPW calculations using Kubo–Greenwood formula for the state with density 8 g/cc, electron temperature $T_e = 2$ kK, and ion temperature $T_i = 2$ kK.

$N_{k\text{-points}}$	r, $\mu\Omega$ m	κ, W/(m K)	ΔE, eV/atom
$4 \times 4 \times 4$	0.32	165.7	2.25
$6 \times 6 \times 6$	0.29	157.6	−1.11
$8 \times 8 \times 8$	0.27	143.1	−0.42
$10 \times 10 \times 10$	0.27	135.4	0.08
$12 \times 12 \times 12$	0.26	132.2	0.007
$8 \times 8 \times 8$ shift	0.27	134.7	0.207
$12 \times 12 \times 12$ shift	0.26	129.0	0

figure 1b. The behavior of DoS is independent of the number of atoms in the system with good accuracy. It can also be noted that the DoS at the Fermi level is not depend on energy in the range of 1 eV. The existing oscillations, clearly visible in the sidebar, are only a consequence of the coarseness of the grid of energy values, which used to reproduce DoS.

During the QMD calculation of thermodynamic properties of copper in the discussed range of densities, electron and ion temperatures were also determined in addition to values of time-averaged thermodynamic potentials for copper phase states in supercells. It turned out that the position of the melting curve changes significantly with the growth of electron temperature and, consequently, pressure at a constant density and ion temperature. Despite the very coarse mesh of ion temperature, it was found that isotherm 2 kK of ion temperature refers to a solid state when the temperature of electrons is 7.5 kK or greater in the whole investigated range of density. Moreover, in the states with a density of 9.4 and 8.8 g/cc and electron temperature equal to 55 kK the solid state is detected at the temperature of ions 4 kK. Conclusions about the phase state of the cell were done according to the calculated pair-correlation functions, which were averaged over all time steps of modeling in NVE ensemble.

It was decided to perform calculations of the electronic kinetic coefficients using DFT and the Kubo–Greenwood formula by two different methods. In the first case, the calculation is continued in code VASP. In the static calculation of the electronic single-particle wave functions, the number of bands was increased to 20 per atom, the cutoff energy was kept equal to the 300 eV, as a condition on the convergence of energy 10^{-5} eV. Data on the convergence of results of calculation with such parameters for the states with 9.4 density g/cc, the electron and ion temperatures of 55 and 2 kK, respectively, are shown in table 1, where we used following designations: N_{at} is a number of atoms in supercell, N_b is a number of empty electrons states, E_{cut} is a planewave cutoff energy, N_{kpt} is a number of points in the Monkhorst–Pack grid. It

Table 3. The convergence in the number of empty electron levels for full-electron calculation for the state with density 9.4 g/cc, electron temperature $T_e = 55$ kK, and ion temperature $T_i = 7.6$ kK.

$N_{k\text{-points}}$	r, $\mu\Omega\,\mathrm{m}$	κ, $\mathrm{W/(m\,K)}$	ΔE, eV/atom
11	1.60	756	133.6
30	1.61	794	0.2
60	1.62	802	0

should be noted that according to table 1, the convergence in the number of particles is not achieved. We will return to this issue when discussing the convergence of the calculations by another method.

Calculation of matrix elements of the momentum operator was based on the previously obtained single-particle electronic wave functions. These elements were calculated for fixed electronic density. After this step, the calculation of dynamic Onsager coefficients was performed, which are then used to find the static values. These values are used to determine all considered in this work electronic kinetic coefficients according to the Onsager relations. The only parameter for which we have to perform the convergence check is the width of the Gaussian function representing the analytical representation of the δ-function in the Fermi "Golden rule". The procedure for determining the correct value for this quantity was carried out as follows. If you take too small width approximation, for the δ-function, it will not be captured by neither of the neighboring electronic level. Accordingly, starting from some value of this width, then it decreases the result of summation by the Kubo–Greenwood formula. On the other hand, if the Gaussian function becomes strongly broadened, there will be errors associated with the fact that the contribution of the nearest levels will have less weight [15]. Accordingly, it is necessary to find an intermediate area in which the aforementioned trends are not evident, and the magnitude of the broadening has no significant effect on the result. The latter is important because the width of the Gaussian function is a computing parameter, not emerging in theoretical formulation, and, consequently, in the ideal case, the influence of this parameter should be negligible. After the investigation, it was found that the optimal value of Gaussian function width is about 0.1–0.15 eV.

In the second case, full-electron approach implemented in the computational code Elk [26] was used. In this code it is possible to define matrix elements using electronic single-particle wave functions calculated by the method of linearized augmented plane waves (LAPW). Also electronic kinetic coefficients according to the Kubo–Greenwood formula can be obtained. The additions in code made for this calculation came down to implementing of expressions for all Onsager coefficients, not only electroconductivity. The procedure of calculation of the chemical potential was added. It is necessary for calculation of L_{12}, L_{21} and L_{22} Onsager coefficients. Now it is possible to set arbitrary width of the δ-function. Initially, it was possible using to calculate the dynamic conductivity by using this code. Since the broadening of the δ-function was fixed at a value of the electron smearing, it was implicitly assumed that the electron temperature will not exceed several thousand Kelvin degrees.

At temperatures of the electrons up to 7.5 kK the grid of Monkhorst–Pack points was used 8x8x8. Data about the convergence at different grids of Monkhorst–Pack points are given in table 2. At higher electronic temperatures (the temperature of electrons 30 kK or greater) the simplified Monkhorst–Pack grid was used with $4 \times 4 \times 4$ points, but the number of unoccupied electronic levels was increased from 11 to 20. The convergence on the last parameter was checked for the point ($\rho = 9.4$ g/cc; $T_e = 55$ kK, $T_i = 2$ kK) to the value of unoccupied levels equal

to 60, and it was shown that the convergence in this parameter are achieved with the required accuracy in 20 unoccupied levels (see table 3). The other parameters of the LAPW calculation were fixed. For the product of the radius of the muffin-tin sphere on the maximal value of the modulus of the electronic wave vector the value of 7.0 was set. The convergence of the total energy and the potential in the Kohn-Sham equation was determined by the values of the differences between the two last iterations 10^{-4} and 10^{-6} Ha, respectively. We have used the local density approximation for the xc-correlation functional in the representation of the Perdew–Wang or Ceperley–Alder, which was used in the calculation with VASP.

Due to large computational complexity of full-electron calculation it was decided to keep only 13 points from the original mesh of density, electron and ion temperatures used in QMD calculations of ionic configurations. At the same time, the minimum of required ensembles of ionic configurations was provided for these points to be able to carry out the procedure of averaging over the configurations.

The check of convergence of full-electron calculation in the number of atoms was performed for copper under the following conditions: the density is 9.4 g/cc, the equilibrium temperature is 2 kK. Here 4 ionic configuration were used, which containing 108, 64, 32 and 27 atoms in cubic supercells. In the first case, the number of Monkhorst–Pack points was reduced to $5 \times 5 \times 5$ because of the extremely high requirements of used memory. All other calculation parameters, discussed above, have not been changed. We can notice that owing to the reduced volume of reciprocal space the density of the Monkhorst–Pack points increases. So the resulting densities of Monkhorst–Pack points in the supercells with 108 and 32 atoms are almost the same. In figure 2 it is shown that the convergence of electrical resistivity or thermal conductivity is not achieved with the increase of the length of supercell edge l. Similar behavior was observed also for calculations with a pseudopotential method in the code VASP 1. In order to ease submission of data for supercells of different sizes, the length of supercell edge l is used on the horizontal axis.

As an explanation for such a behavior of the obtained values for kinetic coefficients on the number of particles, it is possible to suggest the following arguments. We will use the Drude model, which can be used for qualitative estimations of the values of kinetic coefficients for liquid copper at these temperatures according to experimental data (see, e.g., [27]). It is known that at the density and temperature close to specified here, the electrical resistivity of copper is $\rho \sim 0.4$ μOhm m. According to the Drude formula $\rho = m_e(n_e e^2 \tau)^{-1}$ and known data for effective electron mass and the number of electrons in the s-conduction band (equal to the electron mass in vacuum and 2 [11], respectively), it turns out that the average effective time between collisions is about 4.6 ps. Then, estimating the speed of the electrons through Fermi value $v_F = \sqrt{2E_F/m_e}$, where $E_F = 9.25$ eV, we can estimate the mean free path of the electron under these thermodynamic conditions is ~ 8 nm. Thus, the maximum of the linear size of the supercells exactly an order of magnitude less than the estimated mean free path. Immediately, you can specify that currently, the method of quantum molecular dynamics is impossible for a system of $\sim 10^5$ atoms due to the computational limitations.

On the other hand, remaining in the framework of the Drude model, we can try to estimate, are there any conditions in which the first-principles calculation may be carried out by the condition of convergence in the number of particles. Presented in figure 5a results show that resistivity becomes equal to 1 μOhm m at heating to a few tens of thousands Kelvin. In some works [6, 28] on the basis of obtained by DFT calculations partial DoS one conclude that the number of s-electrons with increasing T_e is growing from 1 to 2. The mean free path length is reduced to 2–5 nm, which would require about 600 atoms that are already close to modern computing capabilities, however, this or a greater number of atoms achieved so far only for aluminum [29]. Figure 2 shows that the change of the electrical resistivity and heat conductivity with increasing number of atoms from 32 to 108 achieves approximately 30%. The same fact is

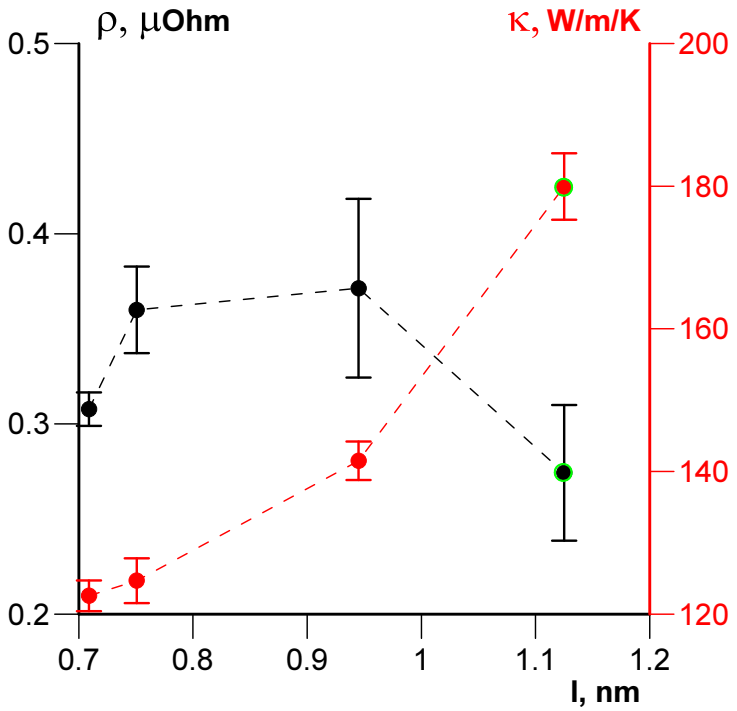

Figure 2. The dependencies of electroresistivity (black points) and heat conductivity (red points) on the linear size of used cubic supercells.

shown in figure 2, where errors shown in this figure correspond only to the contribution of the averaging over the configurations. The error due to convergence in the number of unoccupied levels for a cell with 32 atoms is 0.5 and 6% for resistivity and heat conductivity, respectively. The error from the convergence on the grid points of Monkhorst–Pack is estimated equal to 4 and 7% for this supercell.

In conclusion of this section, the convergence results for the kinetic coefficients in the width of δ-function broadening width are shown. In full-electron calculation, the value of width, which should be used according to the aforementioned criterion, is also ~ 0.1 eV. This conclusion is illustrated by the behavior of electrical resistivity with increase of the width in figure 3a. It can be noted that in full compliance with the work [29] an area of applicable values for width increases with the number of atoms in supercell. Also it is interesting to investigate the behavior of the electrical conductivity with the growth of the discussed parameter. According to figure 3b it was obtained that the heat conductivity starts to grow linearly with the broadening width as $k_W = k_0 + a\delta$, where both the coefficients k_0, a are positive. To verify this statement, the calculations were made at too high width of 2.7 eV. Using the results of these calculation we showed that the linear law remains when the value of δ is many times greater than the one that should be used according to the criterion which is found at the consideration of electrical resistivity. Additionally, the inset shows that the ratio of the values obtained in the calculation and linear asymptotics, comes close to unity, starting with the ~ 0.1 eV, which is the applicable region of values of δ. The error due to the variation of δ can be evaluated equal to 10%.

3. First-principles results

According to the results of the previous section, only 13 thermodynamic states were considered due to the high computational capacity of calculation. These states are differ by density, electron

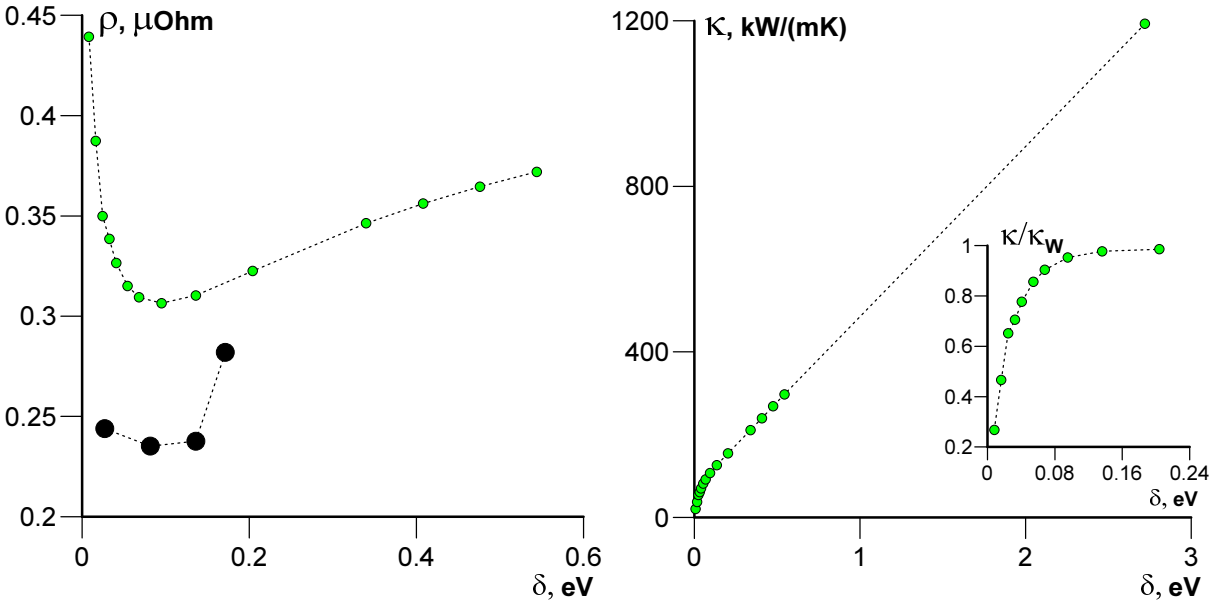

Figure 3. (a) The dependencies of electrical resistivity from δ-function broadening for 108 and 27 atoms (black and green points). (b) Behavior of heat conductivity at different values of δ-function broadening for the supercell with 27 atoms. In the sidebar, these values are divided on the linear asymptotic law $\kappa_W = 74.3 + 411.2\delta$.

or ion temperatures. The results obtained here for density 8 g/cc, electronic temperature up to 55 kK, and different ion temperatures are presented in figure 4. In figure 4a we provided the data for electrical resistivity at different ion temperatures 2 and 7.5 kk, respectively. These data was obtained by full-electron calculations. As we can see in figure 4b, the curves of electronic conductivity are determined using full-electron and pseudopotential calculation agree well with each other.

In addition to the results of direct calculations in figure 4, the curves are drawn for two fittings constructed to reproduce the data for Onsager coefficients at whole ranges of density and both temperatures. The functional form of these fittings are similar to that proposed in the paper [7]. In the case of thermal conductivity and full-electron calculation, the shape of the fitting according to full-electron calculation looks like this:

$$\kappa_{\mathrm{FE}}(\rho, T_e, T_i) = \gamma_0 \frac{T_e^g + \beta_i(\rho_0/\rho)^b}{(1 + \gamma_m T_e^s)(C_i + T_e^d)}. \tag{1}$$

Assuming that electron and ion temperatures are taken in eV, the coefficients in (1) have the following values: $\gamma_0 = 0.888$ W/(m K), $g = 2.239$, $\beta_i = 0.799$, $b = -0.895$, $\gamma_m = 0.00493$, $s = 3.243$, $C_i = 1.215$, $d = 2.035$. Density ρ_0, which is the divisor in the expression (1), is equal to 8 g/cc.

In the case of resistivity functional form is taken as follows:

$$\rho_{\mathrm{FE}}(\rho, T_e, T_i) = \frac{L_{\mathrm{WF}} T_e}{\kappa_{\mathrm{FE}}(\rho, T_e, T_i)}. \tag{2}$$

Here we used the value of Lorentz number L_{WF}, which is equal to 2.44 10^{-8} W Ohm/K^2. In the case of electrical resistivity according to the formula (2) the coefficients used here have the

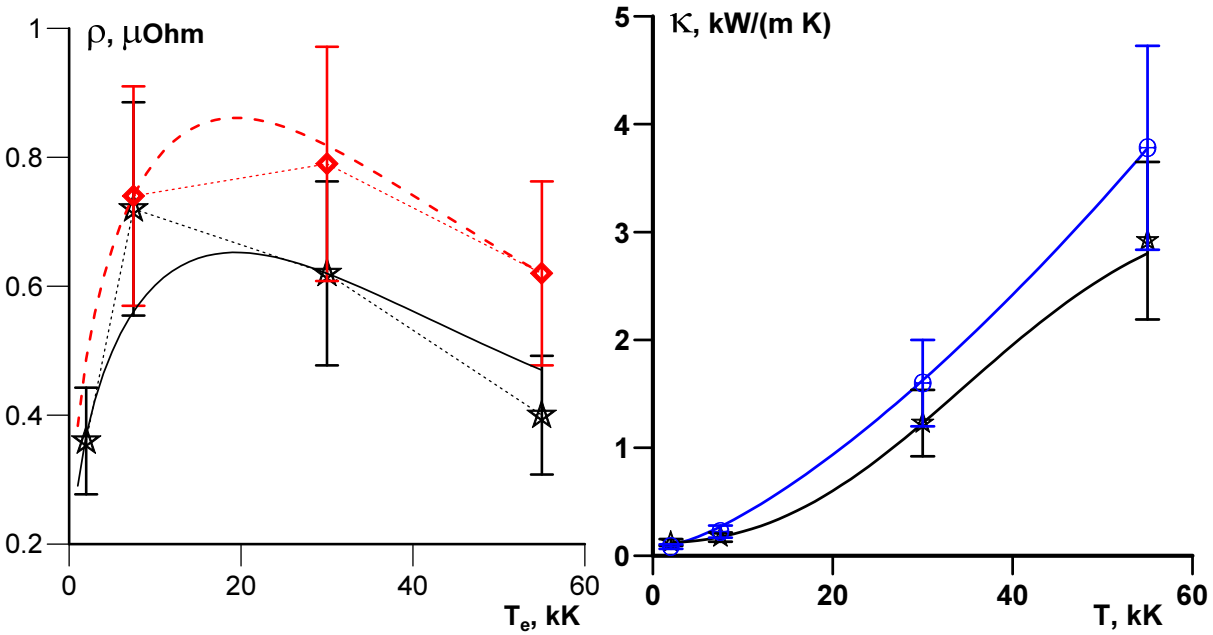

Figure 4. (a) Comparison between calculated data for copper electrical resistivity and analytical fit. Density of copper fixed at 8 g/cc. The data for $T_i = 2$ kK are shown by red diamonds and dashed line. The same results for $T_i = 7.5$ kK correspond to the black stars and line. (b) Two fits for full-electron and pseudopotental calculation (black and blue lines) are compared with the data of calculations used to obtain these fits.

following values: $\tilde{\gamma_0} = 1900$ (μOhm m)$^{-1}$, $\tilde{g} = 1.69$, $\tilde{\beta_i} = 9.085$, $\tilde{b} = -1.085$, $\tilde{\gamma_m} = 9433$, $\tilde{s} = -0.649$, $\tilde{C_i} = 1.221$, $\tilde{d} = 1.888$. This choice of functional form is based on the fact that according to [13] the Wiedemann–Franz law is fulfilled at temperatures up to 10 kK with a good accuracy. Of course, in the case of copper and higher temperatures the agreement may be worse. However, independent selection of the coefficients in (2) which was carried out without any assumption about the validity of the Wiedemann–Franz law, allows us to describe the behavior with a precision of 6%. Here the accuracy is defined using the data for the standard deviation in all points is calculated directly. As for thermal conductivity, this error equal to 7% according to the formula (1).

4. Semi-analytical model for transport properties

Here we provide the description of semi-analytical model constructed on the principles similar to used in the model presented in the work [30, 31].

Electron heat conductivity in time relaxation approximation can be written as

$$\kappa_e = \frac{1}{3}\frac{C_v v^2}{\nu}.$$

Here C_v is the electron heat capacity for s-band electrons at fixed volume, v^2 is the mean square of their velocity, and $\nu = 1/\tau$ is the mean frequency of collisions between electrons and all types of scatterers, which is a probability of collision in time unit at given relaxation time τ. After selection of electron-electron collisions with effective frequence $\nu_{\rm se}$ and electron-ion collisions with effective frequency $\nu_{\rm si}$, we can sum their reciprocal values using Matthiessen rule and the

result is:

$$\frac{1}{\kappa_e} = \frac{1}{\kappa_{\rm se}} + \frac{1}{\kappa_{\rm si}},$$

Here $\kappa_{\rm se}$ and $\kappa_{\rm si}$ are coefficients for heat conductivity of s-electrons due to electron-electron and electron-ion collisions. By other hand, we can separate the contributions of collisions of s-electrons with s-($\nu_{\rm ss}$) and d-electrons ($\nu_{\rm sd}$). That gives

$$S_e(T_e, x) = \frac{1}{\kappa_{\rm se}} = \frac{1}{\kappa_{\rm ss}} + \frac{1}{\kappa_{\rm sd}}. \tag{3}$$

The reciprocal value of heat conductivity has its own name which is thermal resistivity S_e and can be calculated using time relaxation approximation for Boltzmann kinetic equation for ss and sd scattering processes [10]. This solution is a function of electron temperature T_e and relative density $x = n/n_0$, The last is equal to ratio between atom concentration and atom concentration at low temperature which is close to zero.

In the case of low temperatures

$$\kappa_{\rm se} = S_e^{-1}(T_e, x) \sim n k_B \frac{k_B T_e}{\varepsilon_F} v_F^2 \frac{\hbar}{\varepsilon_F} \left(\frac{\varepsilon_F}{k_B T_e}\right)^2 \sim n k_B \frac{\hbar v_F}{p_F} \frac{\varepsilon_F}{k_B T_e} \sim \hbar k_B \frac{n}{m^*} \frac{\varepsilon_F}{k_B T_e}.$$

Here k_B is Boltzmann constant, ε_F, v_F, p_F are Fermi energy, velocity and momentum, respectively, and all of them are depend on density, m^*—s-electron effective mass.

In suggestion that electron effective mass is constant, Fermi energy ε_F (the difference between the energy where all 11 valence band states are filled and the bottom of s-band) grows with atomic concentration n as $\varepsilon_F \sim n^{2/3}$. Thus $\varepsilon_F = \varepsilon_{F0} x^{2/3}$, where ε_{F0} is a Fermi energy at zero pressure. Therefore, at low temperature limit

$$\kappa_{\rm se} \sim n \frac{\varepsilon_F}{k_B T_e} \sim x \frac{\varepsilon_F}{k_B T_e}, \quad S_e(T_e, x) \sim n^{-1} \frac{k_B T_e}{\varepsilon_F} \sim x^{-1} \frac{k_B T_e}{\varepsilon_F}.$$

Thus we can fit these results of calculation of thermal resistivity (3) by such an expression:

$$S_e(T_e, x) = x^{-1} \frac{a_0 t}{1 + b_0 \sqrt{t} + b_1 t + b_2 t^2}. \tag{4}$$

Here we denote $t = 6 k_B T_e / \varepsilon_F = 6 k_B T_e / (\varepsilon_{F0} x^{2/3})$, and coefficients

$$a_0 = 3.80284 \times 10^{-4}, \quad b_0 = -1.99157, \quad b_1 = 1.35301, \quad b_2 = 0.0395385$$

give the value S_e in m K/W. Due to the fact that S_e is defined only by electronic subsystem, the expression for this value does not depend on the copper phase state (solid or liquid).

Now we consider the role of electron-ion collisions in heat conductivity determination. We should investigate the cases of solid and liquid phases separately. In the solid state the contribution of electron-ion collisions can be approximated by the formula:

$$\kappa_{\rm si} \sim C_v v \lambda_{\rm si} \sim n k_B C(t) v_F \lambda_{\rm si}.$$

In the multiplication of s-electron heat capacity and mean square of s-electron velocity $v = (v_F^2 + 3 k_B T_e / m^*)^{1/2} = v_F (1 + t/4)^{1/2}$, we separate the function $C(t)$ which depends on dimensionless parameter t. This function at $x = 1$ can be calculated according to [30] and the results are appoximated by the expression:

$$C(t) = \frac{t(1 + 11.202 t^2)}{1 + 3.34579 t^{2.04855}}. \tag{5}$$

Mean free path at s-electron collision with phonons in solid phase is $\lambda_{\rm si} = 1/(n\Sigma)$. The effective cross section is

$$\Sigma \sim u_0^2 \frac{T_i}{\theta},$$

where $u_0^2 \sim \hbar^2/(Mk_B\theta)$ is a mean squared amplitude of zero oscillations of atoms with mass M, and θ is a Debye temperature. Thus, we have for $\lambda_{\rm si}$

$$\lambda_{\rm si} \sim \left(n \frac{T_i}{\theta} \frac{\hbar^2}{Mk_B\theta} \right)^{-1} \sim \frac{Mk_B}{\hbar^2 T_i} \frac{\theta^2}{n} \sim \frac{\theta^2}{nT_i}.$$

Debye temperature as function of density can be determined using some analytical results for thermodynamics of a metal in solid state. We can give a representation of cold curve [32,33] for copper not far from the equilibrium at $T = 0$ density in the following way:

$$p_c(v) = \frac{A}{v} \left(\left(\frac{v_0}{v} \right)^a - \left(\frac{v_0}{v} \right)^b \right). \tag{6}$$

v is a volume per atom, v_0 is the value of v at zero pressure, $a > b$.

Debye energy is $k_B\theta = \hbar s k_D$, where Debye wavenumber $k_D = (6\pi^2 n)^{1/3}$ and sound velocity $s \propto \sqrt{K/(Mn)}$. Bulk modulus K can be found using the defined cold curve (6)

$$K = -v\frac{dp_c}{dv} = \frac{A}{v} \left((a+1) \left(\frac{v_0}{v} \right)^a - (b+1) \left(\frac{v_0}{v} \right)^b \right).$$

Thus, Debye temperature squared is

$$\theta^2(x) \propto x^{2/3} y(x), \quad y(x) = \frac{(a+1)x^a - (b+1)x^b}{a-b}.$$

Here $x = v_0/v$. Parameters a and b can be defined with the help of cold pressure curve from [32,33], where the density at zero pressure and temperature is $\rho_0 = 9.018$ g/cc. Therefore,

$$a = 1.826, \quad b = 1.788.$$

To consider relative densities in the range $x < 1$ the function $y(x)$ should be replaced on the close to it function $\bar{y}(x)$, which values are always greater than zero:

$$\bar{y}(x) = \frac{(1 + c_{\rm ab})x^{2a+1}}{1 + c_{\rm ab}x^{a+1}}, \quad \theta^2(x) \propto x^{2/3}\bar{y}(x) \tag{7}$$

with $c_{\rm ab} = (a-b)/(b+1)$. After introduction of function $\bar{y}(x)$ (7) mean free path for electron-phonon collisions is

$$\lambda_{\rm si} \propto [\bar{y}(x)x^{-1/3}]T_i^{-1},$$

and heat conductivity due to electron-phonon collisions

$$\kappa_{\rm si}^{\rm sol} \propto x\bar{y}(x)C(t)/T_i.$$

The experimental value of heat conductivity on zero pressure isobar at room temperature $T_{\rm rt} = 0.298$ kK and equilibrium density $\rho_{\rm rt} = 8.96$ g/cc is equal to $\kappa_{\rm rt} = 401$ W/(m K). Thus, thermal conductivity due to electron-phonon collisions finally has the form:

$$\kappa_{\rm si}^{\rm sol} = \kappa_{\rm rt}(x/x_{\rm rt})(\bar{y}(x)/\bar{y}(x_{\rm rt}))(T_{\rm rt}/T_i)C(t)/C(t_{\rm rt}). \tag{8}$$

($t_{\rm rt} = 6k_B T_{\rm rt}/(\varepsilon_{F0} x_{\rm rt}^{2/3})$). Then thermal conductivity in the solid state can be calculated as

$$\kappa_{\rm sol} = \frac{1}{S_e(T_e, x) + 1/k_{\rm si}^{\rm sol}}. \tag{9}$$

Also we can construct the similar expression of heat conductivity of liquid copper in two-temperature state. Electron-electron contribution are not effected by melting and save its form S_e. We suggested that the mean free path for electrons λ_l due to electron-ion scatterings in liquid can be expressed in the following way: $\lambda_l = n_0^{-1/3} W(T_i) x^\beta$. Omitting some actions with λ as for solid phase, we have for heat conductivity $\kappa_{\rm ei}^l$ due to electron-ion collisions

$$\kappa_{\rm ei}^l(T_e, T_i, x) \propto x C(t) x^{1/3} W(T_i) x^\beta.$$

By other side, electroresistivity in Drude model

$$r(T_i, x) = \frac{p_F}{n e^2 \lambda_l} = \frac{(3\pi^2)^{1/3}}{2\pi} R_0 \frac{n_0^{1/3}}{n^{2/3} W(T_i) x^\beta} = \frac{r_0}{x^{2/3} W(T_i) x^\beta}.$$

Here $r_0 = (3\pi^2)^{1/3} R_0/(2\pi) n_0^{-1/3} = 3254$ nOhm m, $R_0 = h/e^2 = 25812.8$ Ohm is the quantum of electrical resistivity. Using designations $\gamma = \beta + 2/3$, we have

$$r(T_i, x) = \frac{r_0}{W(T_i) x^\gamma}.$$

We fixed γ equal to 2. We can determine $W(T)$ using known experimental dependence $r_l(T)$ for copper electroresistivity on the temperature on the boiling curve $x_l(T)$, so we can write

$$W(T) = \frac{r_0}{r_l(T) x_l^\gamma(T)}.$$

If we introduce the values $\tau_l = \sqrt{(T_c - T)/T_c}$ and $\tau_m = T - T_m$, where $T_c = 7890$ K is a critical temperature, $T_m = 1.36$ kK is a melting temperature at atmospheric pressure, then relative density on the boiling curve $x_l(T)$ can be written as

$$x_l(T) = 0.247235 + 0.705936\tau_l(1 - 0.115883\tau_l^2 + 0.113314\tau_l^4). \tag{10}$$

And the behavior of electroresistivity on this curve (nOhm m):

$$r_l(T) = 210.1 + (1.5\tau_m + 4800\tau_m^2)/(\tau_m^2 + 3300^2). \tag{11}$$

This expression is the same as known experimental data. At high temperatures, it becomes equal to the limit for strongly disordered systems. Thus with the use of (5), (10), (11) and we can obtain heat conductivity for liquid copper due to electron-ion collisions in the form:

$$\kappa_{\rm ei}^l(T_e, T_i, x) = 138 \frac{C(t)}{C(t_m)} \frac{r_l(T_m)}{r_l(T_i)} \left(\frac{x}{x_l(T_m)}\right)^{2/3} \left(\frac{x}{x_l(T_i)}\right)^\gamma. \tag{12}$$

Here $t_m = 6k_B T_m/(\varepsilon_{F0} x_l^{2/3}(T_m))$. The net heat conductivity for liquid phase can be expressed using $\kappa_{\rm ee}$:

$$\frac{1}{\kappa_l} = S_e + \frac{1}{\kappa_{\rm ei}^l}. \tag{13}$$

5. Role of electron-electron collisions

Calculations, carried out using semi-analytical models, allow considering partial contributions to the electronic conductivity which is related with electron-electron and electron-ion collisions. In the case of first-principles calculations we can't do that, and the question of how much, for example, the contribution of electron-electron collisions remains an open case. The functional of the electronic density, which is determined by minimization of ground state energy, contains the contribution of electron correlations in the xc-functional (see, e.g., [5]). Among the calculations performed in preparation for this work, there were calculations, which differed only in the use of some well-known xc-functionals. This was done using the VASP code where the PAW pseudopotentials exists with LDA and PBE forms of xc-contribution to electronic density functional. The changes caused by the usage of different xc-functionals are found as negligible in the results for heat conductivity (∼1-2%). For this reason, these data are not presented.

Based on data from semi-analytical models in electron temperatures of the order of several eV, the effective frequency of electron-electron collisions, obtained as a sum of two types of collisions (ss+sd) becomes of the same order as effective frequency of electron-ion collisions. Thus, we may doubt on the correctness of consideration of electron-electron collisions in first-principles calculations where the difference between the calculated data for the thermal conductivity is independent from used xc-functional. The usage of these two xc-functionals effect on any calculated properties of copper, such as a cold curve or DoS. It would be the right choice to check how the calculation results will change, if the assumption of zero contribution of electron-electron collisions in QMD calculations is true. In this case, we can perform a summation of the result of QMD calculations and semianalytically obtained electron-electron contribution according to the Matthiessen rule:

$$\frac{1}{\kappa} = \frac{1}{\kappa_{\mathrm{FE}}} + \frac{1}{\kappa_{\mathrm{ee}}}. \tag{14}$$

The result of full-electron calculation is in the form of fit (1). An analytical expression for electron-electron contribution is the result of fitting of the tabular data in the solution of the Boltzmann equation in the relaxation time approximation.

In accordance with the Drude model, we should take into account the contribution of interband (sd) collisions which was provided by Matthiessen rule:

$$\rho = \rho_{\mathrm{FE}} + \rho_{\mathrm{sd}}. \tag{15}$$

Here ρ_{FE} is the electrical resistivity according to the formula (2). A contribution of sd-collisions is detected as weakly density dependent, and we neglected this dependence. Then for the density range of 7.6-9.4 g/cc it can be written [11]:

$$\rho_s d(T_e) = \frac{0.0942 T_e^2}{1.2 + 0.1751 T_e^2}. \tag{16}$$

According to the formula (16), the contribution to the interband electron collisions bands is saturated in the studied temperature range (temperature of electrons in the formula (16) is taken in eV).

In figure 5, it is shown that the results of summation by the formula (16) do not change in contrast to the data of full-electron calculation which are decreased at temperatures greater than 2 eV. The results presented in figure 5b, show that the resulting growth of thermal conductivity becomes slower with increasing of electron temperature. Unlike to the case of electrical resistivity produced the difference produced by the correction is significant. On the one hand, these first-principles calculations by full-electron and pseudopotential methods are in good agreement. On the other hand, as will be seen below, the data after the correction are in good agreement with the predictions of semi-analytical model which is not related with the data of QMD calculations of the kinetic coefficients according to its basic statements.

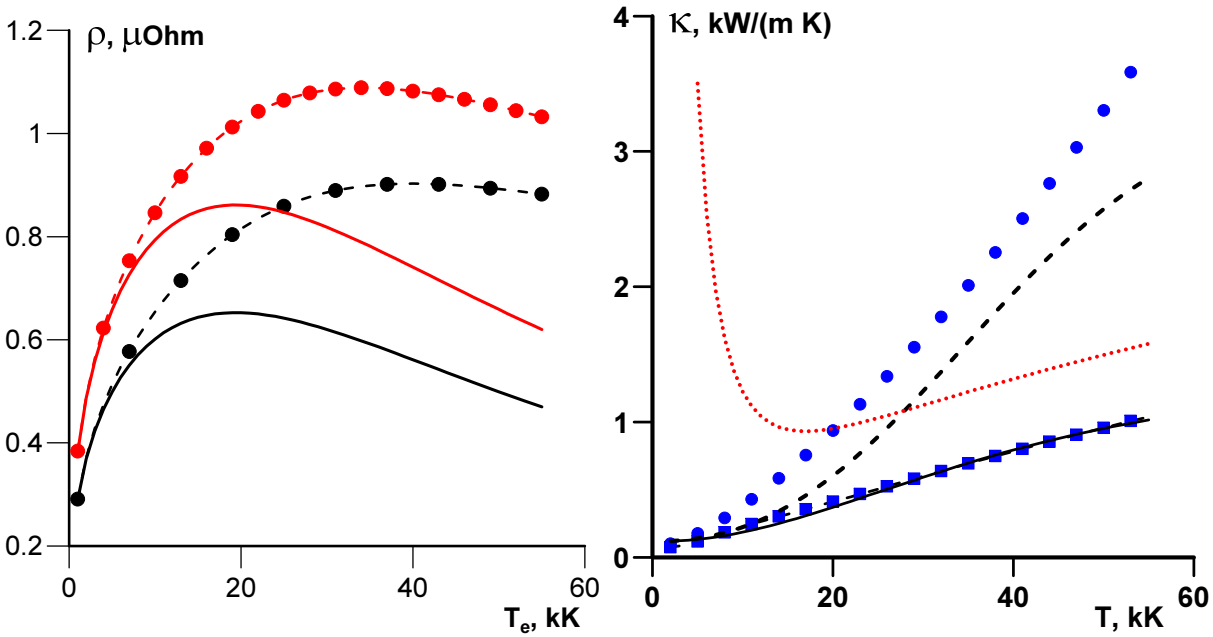

Figure 5. (a) Electrical resistivity as a function of electron temperature at fixed ion temperature values: 2 kK (black lines) and 7.5 kK (red lines). The same data but with contribution of electron-electron collisions by formula (16) are shown by dashed lines with circles (b) Electron heat conductivity as a function of electron temperature. The results of full-electron (black dashed line) and pseudopotential (blue circles) were corrected on the value of electron-electron contribution (red points). The corrected data are shown by solid black line (full-electron calculations) and blue squares (pseudopotential).

6. Comparison of QMD data with semiempirical model

In figure 6a, the result of comparison for the data on electrical resistivity as a function of equilibrium temperature, is presented. It is evident that analytical fit defined using the data of calculations of full-electron approach is in good agreement at a temperature of 2 kK with the result of the experiment [27], and wide-range data model [34] for copper at 10 kK. In the latter case, the agreement for the densities of 7.6 and 9.4 g/cc has been shown. But at low temperatures the experimental value of the electrical resistivity at the melting point is not reproduced. Although the density corresponding to this point equal to 8 g/cc, the experimental value for 1.36 kK lies significantly below the obtained values for 7.6 g/cc. Also the obtained results are located above the predicted values from the other wide-range plasma model [35, 36].

In figure 6b, the data for the heat conductivity of copper as a function of electron temperature are shown. As we can see after the correction for electron-electron contribution, the results of full-electron and pseudopotential calculations become almost indistinguishable. They agree well with the curve calculated in accordance with semi-analytical model for liquid copper. The thermal conductivity of a solid copper based on the results of the same model can be significantly higher. The result from the work [37], which was obtained by the determination of parameters of phenomenological formula [7] using FP-LMTO calculations, predict a drop of thermal conductivity with increasing electronic temperature, and gives much smaller values for this quantity.

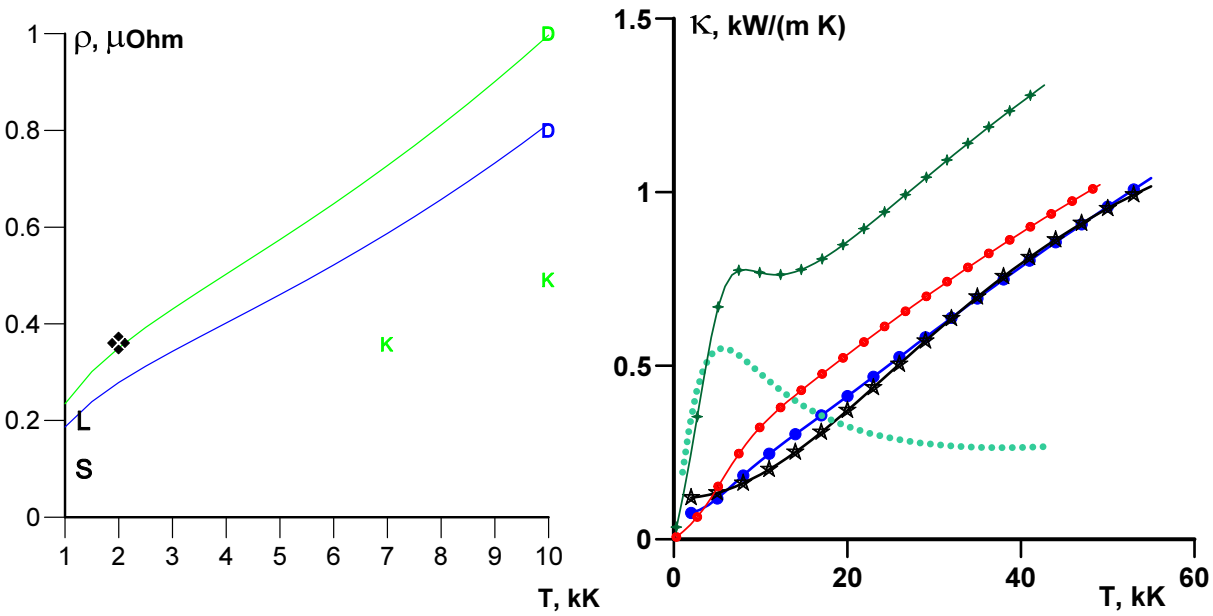

Figure 6. (a) The results for the analytical fit of full-electron calculation of electrical resistivity as a function of equilibrium temperature are shown by blue (density 9.4 g/cc) and green (7.6 g/cc) lines. The experimental result obtained at temperature 2 kK on binodal curve (local value of density is $\sim$ 7.5 g/cc) is shown by black diamond. The experimental points for electrical resistivity of copper before and after melting at atmospheric pressure are shown by letters "S" and "L". The predictions of Lee–More–Desjarlais model [34] are shown by blue (9.4 g/cc) and green (7.6 g/cc) letters "D". The results for temperatures 7 and 10 kK and density 7.6 g/cc obtained using BKL model are denoted by green letters "K". (b) The results of discussed calculations and models for electron heat conductivity at density 8 g/cc. The data of analytical fits for full-electron and pseudopotential calculations are shown by black line with stars and blue line with circles, respectively. The predictions of semi-analytical model of copper transport properties refer to solid (green line with crosses) and liquid (red line with circles) states. Also the result of the work [37] based on the semi-analytical approach [7] corresponds to green dotted line.

7. Conclusions

For liquid homogeneously stretched/compressed copper with heated electrons the data about a behavior of electronic heat conductivity and electrical resistivity are obtained using QMD calculations and the Kubo–Greenwood formula. The study of convergence of results calculated by the method of pseudopotential and full-electron approaches is provided. Presented semi-analytical model, introduced independently on the calculations, predict the values of the transport coefficients for copper in the same ranges of thermodynamic parameters. We can suggest the statement that the correction of first-principles calculations by the contribution of electron-electron collisions should be made. Results of analytical fits for corrected data of first-principles calculations and data semi-analytical model are in good agreement.

Acknowledgments

The following authors PYV, MKP, and INA are grateful to the Russian Foundation for Basic Research for support (grant 16-02-00864). We are also grateful to the FAIR-Russian Research Center, the State Atomic Energy Corporation "Rosatom", the Helmholtz Association, the

Ministry of Education and Science of the Russian Federation (project No. 3.522.2014/K). We acknowledge the Supercomputer Centre JIHT RAS for providing computing time.

References

[1] Ogitsu T, Ping Y, Correa A, Cho B, Heimann P, Schwegler E, Cao J and Collins G W 2012 *High Energy Density Phys.* **8** 303
[2] Cho B I, Engelhorn K, Correa A A, Ogitsu T, Weber C P, Lee H J, Feng J, Ni P A, Ping Y, Nelson A J, Prendergast D, Lee R W, Falcone R W and Heimann P A 2011 *Phys. Rev. Lett.* **106** 167601
[3] Clerouin J, Renaudin P, Laudernet Y, Noiret P and Desjarlais M 2005 *Phys. Rev.* B **71** 064203
[4] Surh M, III T B and Yang L 2001 *Phys. Rev. Lett.* **86** 5958
[5] Reinholz H, Ropke G, Rosmej S and Redmer R 2015 *Phys. Rev.* B **91** 043105
[6] Bevellon E, Colombier J P, Recoules V and Stoian R 2014 *Phys. Rev.* B **89** 115117
[7] Anisimov S I and Rethfeld B 1997 *Proc. SPIE* **3093** 192
[8] Ivanov D and Zhigilei L 2003 *Phys. Rev.* B **68** 066114
[9] Inogamov N A and Petrov Yu V 2010 *J. Exp. Theor. Phys.* **110** 446
[10] Petrov Yu V, Inogamov N A and Migdal K P 2013 *JETP Lett.* **97** 20
[11] Migdal K P, Il'nitsky D K, Petrov Yu V and Inogamov N A 2015 *J. Phys.: Conf. Ser.* **653** 012086
[12] Desjarlais M, Kress J and Collins L 2002 *Phys. Rev.* B **66** 025401
[13] Recoules V and Crocombette J P *Phys. Rev.* B **72** 104202
[14] Norman G, Saitov I, Stegailov V and Zhilyaev P 2013 *Contrib. Plasma Phys.* **53** 300
[15] Knyazev D V and Levashov P R 2014 *Phys. Plasmas* **21** 073302
[16] Levashov P R, Sin'ko G V, Smirnov N A, Minakov D V, Shemyakin O P and Khishchenko K V 2010 *J. Phys.: Condens. Matter* **22** 505501
[17] Sin'ko G V, Smirnov N A, Ovechkin A A, Levashov P R and Khishchenko K V 2013 *High Energy Density Phys.* **9** 309
[18] Holst B, Recoules V, Mazevet S, Torrent M, Ng A, Chen Z, Kirkwood S E, Sametoglu V, Reid M and Tsui Y Y 2014 *Phys. Rev.* B **90** 035121
[19] Minakov D V, Levashov P R, Khishchenko K V and Fortov V E 2013 *J. Appl. Phys.* **115** 223512
[20] Minakov D V and Levashov P R 2015 *Phys. Rev.* B **92** 224102
[21] Migdal K P, Petrov Y V, Il'nitsky D K, Zhakhovsky V V, Inogamov N A, Khishchenko K V, Knyazev D V and Levashov P R 2016 *Appl. Phys.* A **122** 408
[22] Kresse G and Furthmuller J 1996 *Phys. Rev.* B **54** 11169
[23] Kresse G and Joubert D 1999 *Phys. Rev.* B **59** 1758
[24] Kodolov V I, Zaikov G E and Haghi A K 2014 *Nanostructures, Nanomaterials, and Nanotechnologies to Nanoindustry* AAP Research Notes on Nanoscience and Nanotechnology (Apple Academic Press)
[25] Errandonea D 2013 *Phys. Rev.* B **87** 054108
[26] Elk is an all-electron full-potential linearised augmented-planewave (fp-lapw) code released under either the gnu general public license (gpl) or the gnu lesser general public license (lgpl). elk code is available on http://elk.sourceforge.net
[27] Matula R A 1979 *J. Phys. Chem. Ref. Data* **8** 1147
[28] Stegailov V and Zhilyaev P 2015 *Contrib. Plasma Phys.* **10** 1
[29] Knyazev D V 2015 *Calculation of electroresistivity, heat conductivity and optical properties of dense plasmas on the basis of quantum molecular dynamics and Kubo–Greenwood formula* Ph.D. thesis Joint Institute of High Temperature RAS
[30] Petrov Yu V, Migdal K P, Inogamov N A and Zhakhovsky V V 2015 *Appl. Phys.* B **119** 401
[31] Petrov Yu V, Inogamov N A, Anisimov S I, Migdal K P, Khokhlov V A and Khishchenko K V 2015 *J. Phys.: Conf. Ser.* **653** 012087
[32] Khishchenko K V 2004 *Tech. Phys. Lett.* **30** 829
[33] Khishchenko K V 2015 *J. Phys.: Conf. Ser.* **653** 012081
[34] Desjarlais M 2001 *Contrib. Plasma Phys.* **41** 267
[35] Bakulin Yu D, Kuropatenko V F and Luchinskiy A V 1976 *Tech. Phys.* **46** 1963
[36] Oreshkin V I, Baksht R B, Labetsky A Y, Rousskikh A G, Shishlov A V, Levashov P R, Khishchenko K V and Glazyrin I V 2004 *Tech. Phys.* **49** 843
[37] Loboda P, Smirnov N, Shadrin A and Karlykhanov N 2011 *High Energy Density Phys.* **7** 361